

Black nickel electrodeposition from a modified Watts bath

MAGDY A. M. IBRAHIM

*Department of Chemistry, Faculty of Science, Ain Shams University, Abbassia, Cairo, Egypt
(E-mail: imagdy1963@hotmail.com)*

Received 21 February 2005; accepted in revised form 8 September 2005

Key words: black nickel, current efficiency, electrodeposition, potentiodynamic, Tafel lines

Abstract

Black nickel coatings were electrodeposited on to steel substrates from a Watts bath containing potassium nitrate. The best operating conditions necessary to produce smooth and highly adherent black nickel were found to be $\text{NiSO}_4 \cdot 6\text{H}_2\text{O}$ 0.63 M, $\text{NiCl}_2 \cdot 6\text{H}_2\text{O}$ 0.09 M, H_3BO_3 0.3 M and KNO_3 0.2 M at pH of 4.6, $i = 0.5 \text{ A dm}^{-2}$, $T = 25^\circ\text{C}$ and $t = 10$ min. The modified Watts bath has a throwing power (TP) of 61%, which is higher than that reported, not only for nickel, but also for many other metals electrodeposited from different baths. The potentiostatic current–time transients indicate instantaneous nucleation. X-ray diffraction (XRD) analysis shows that the black nickel deposit is pure metallic nickel with Ni(111) preferred orientation.

1. Introduction

Black nickel is of distinctive appearance and is particularly suitable for articles such as camera fittings, hardware, optical and electrical instruments. Another application of the process is in the manufacture of metal name plates, in which it is used for producing a black finish on the etched background [1].

Coatings formed from black metals (i.e., black nickel, black chromium, black cobalt) have been shown to form fairly efficient solar collector surfaces [2–5]. Black nickel, when plated onto a satin or matt surface, is a selective absorber and is being considered as a suitable coating for solar energy collectors [6]. Several techniques, such as chemical conversion and/or thermal oxidation of metallic films and electrodeposition, are currently used to achieve such spectrally selective, black-metal, solar absorber surfaces. However, the desired characteristics of the metallic coating may be better controlled by direct electrodeposition. In order to achieve control and reproducibility for the coating to qualify as an industrially useful material, the deposition process must be properly characterized.

The most used black nickel electrodeposition processes have been based on an electrolyte containing nickel, zinc, thiocyanate and ammonium ions, though Rochelle salt is sometimes used in place of thiocyanate [7]. Black nickel deposits probably consist largely of nickel sulphide and zinc together with free nickel. Serfass et al. [8] have explained the mechanism of black nickelling as follows. At the start of the electrolysis, nickel and either nickel–zinc alloy or zinc deposit and hydrogen is evolved. The evolution of hydrogen then decreases somewhat due to its overvoltage on these

metals, but the increase in alkalinity at the metal solution interface results in the formation of nickel–ammonium and zinc–ammonium ions. The deposition of metals from their ammonia complexes is more difficult [9] than from the free metal ions and then the reduction of the thiocyanate becomes the preferred reaction. The deposition of black nickel sulphide ion and the nickel–ammonium ions on the surface of the metals lowers the overvoltage of hydrogen to nearly the same value as at the start of the process, and the cycle is then repeated.

The present work aims to develop a new bath for producing black nickel coatings from a Watts bath containing potassium nitrate. In addition, the study aims to understand the mechanism of black nickel electrodeposition.

2. Experimental details

The electrodeposition of black nickel was carried out using a bath containing: $\text{NiSO}_4 \cdot 6\text{H}_2\text{O}$ 0.63 M, $\text{NiCl}_2 \cdot 6\text{H}_2\text{O}$ 0.09 M, H_3BO_3 0.3 M and with different concentrations of KNO_3 . All the plating baths and reagents were made from Analar chemicals, without further purification, and doubly distilled water. For electrodeposition, a steel sheet of dimension 2.5×3.0 cm was used as cathode. A platinum sheet of dimensions, 2.5×3.0 cm, was used as anode. The plating cell was a rectangular Perspex trough (10×3 cm) provided with vertical grooves, on each of the side walls, to fix the electrodes. Before each run the steel cathode was mechanically polished with different grades of emery papers (600, 800, 1000 and 1500) then

washed with distilled water rinsed with ethanol and weighed. Direct current was supplied by a d.c. power supply unit (GPS-3030D). The cathodic current efficiencies CCE were determined with the help of a Cu-coulometer ($CCE\% = w_{\text{exp}}/w_{\text{th}}$) where w_{exp} is the weight of the deposit obtained experimentally and w_{th} is the weight of the deposit calculated theoretically according to Faraday's law. Electrodeposition was carried out for 10 min in each case.

The percentage TP of the solution was measured using a Haring-Blum rectangular Perspex cell (3.0 cm width, 13 cm long with 2.5 cm depth) fitted with one anode between two parallel steel cathodes where the ratio of the far to the near distance was 5:1. This was calculated from Field's formula [10]:

$$TP = (L - M)/(L + M - 2) \times 100 \quad (1)$$

where L is the ratio of the cathode distance to the anode distance (far to near 5:1) and M is the ratio of the weight of the deposited metal on the near to the weight of the deposited metal on the far cathode. The values of M were measured as a function of L over a wide range of linear ratios varying between 1:1 and 5:1. The throwing index (TI) was considered as the reciprocal of the slope of the M against L plot.

Potentiodynamic cathodic polarization curves were recorded using steel substrates by sweeping the potential from the rest potential in the negative direction with scan rate of 20 mVs^{-1} . A potentiostat/Galvanostat (EG&G model 273) controlled by a computer was used for all the electrochemical measurements. All potentials were measured relative to a saturated calomel electrode (SCE). To avoid contamination, the reference electrode was connected to the working cathode via a bridge provided with a Luggin-Haber tip and filled with the solution under test.

The crystalline structure of the black nickel deposited on steel from the modified Watts bath was examined by XRD using a Philips PW 1390 diffractometer (40 kV, 20 mA) with Ni filter and CuK_α radiation.

3. Results and discussion

The black nickel deposits were obtained by modifying the composition of an electrolytic bath for white nickel production (Watts bath) through the addition of small amount of potassium nitrate. Preliminary experiments were carried out to find the effect of KNO_3 addition on Ni electrodeposition. It is found that a concentration of KNO_3 less than 5×10^{-3} is insufficient to produce black deposits. However, starting from 1×10^{-2} , black Ni deposition begins but with low cathodic current efficiency ($\approx 40\%$). Moreover, addition of 0.2 M KNO_3 produces a compact and smooth black nickel deposit which completely covers the entire surface with acceptable current efficiency (58%). Therefore, the best bath composition for producing sound black nickel deposits was found to be: $\text{NiSO}_4 \cdot 6\text{H}_2\text{O}$ 0.63 M , $\text{NiCl}_2 \cdot 6\text{H}_2\text{O}$

0.09 M , H_3BO_3 0.3 M and KNO_3 0.2 M and this bath was used for further investigations.

No evidence of cracking or flaking was seen when the test specimens were immersed for 15 min in boiling water. The black nickel finish showed no discolouration.

3.1. Cathodic current efficiency

The CCE of nickel deposition with and without addition of KNO_3 is shown in Figure 1. Without addition of KNO_3 the CCE is nearly 100%. However, addition of an increasing amount of KNO_3 decreases the CCE% to a minimum value (CCE = 40%) 0.04 M , which then increases again with increasing KNO_3 concentration and finally levels off at 58%. This means that the CCE of black nickel electrodeposition depends strongly on KNO_3 concentration.

It is likely that an interaction between newly deposited nickel and nitrate ions in solution is occurring. This interaction may involve a direct redox reaction and/or nitrate reduction on the surface of the nickel nuclei. The former reaction would consume the nickel deposit, and the latter would provide electrons to the external circuit.

White nickel formation may proceed as follows:



Black nickel deposition may proceed according to the following electrochemical (3 and 5) and chemical reaction (4):

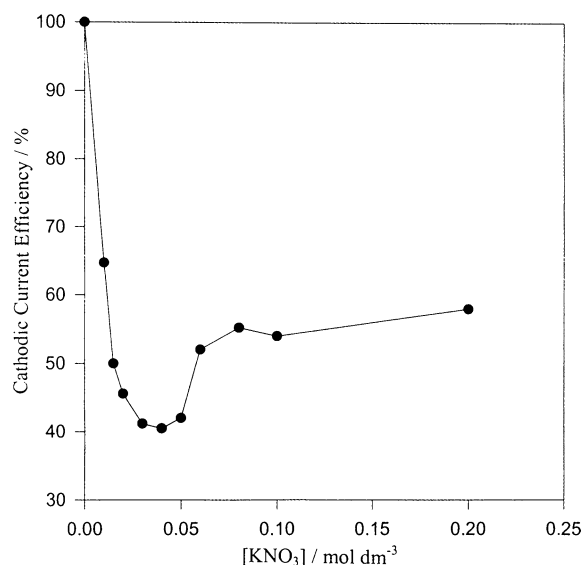
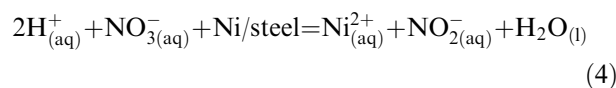
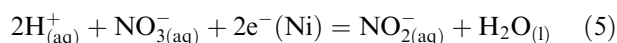


Fig. 1. Cathodic current efficiency against KNO_3 concentrations for nickel electrodeposition.

considering simultaneous nitrate reduction during the cathodic process according to the following reaction



The formation of black nickel films was indeed obtained directly after Ni^{2+} reduction from the aqueous solution containing NO_3^- .

Together or separately, these reactions explain the low nickel efficiency recorded for black nickel formation.

The influence of bath temperature on CCE for black nickel deposition from the modified Watts bath at pH 4.6 and at a current density of 0.5 A dm^{-2} is shown in Table 1. Under such operating conditions ($t = 10 \text{ min}$), the current efficiency reached a maximum value (67%) at 35°C and then decreased with further increase in temperature. The remainder of the studies were carried out at a preferred room temperature of 25°C . One of the most important operating conditions is the applied current density. The relation between the deposition current density and the CCE from the modified Watts bath is given in Figure 2. The CCE of black nickel deposition increases with increasing current density, reaching a maximum value (CCE = 58%) at 0.5 A dm^{-2} and then decreasing slightly as a result of hydrogen evolution. The influence of deposition time on the CCE% was investigated and the data reveal that the CCE increases with increasing deposition time (Table 1). For example, increasing the time of deposition from 5 to 15 min improves the CCE from 28 to 60.5%.

3.2. Potentiodynamic cathodic polarization curves and Tafel lines

Figure 3 shows typical cathodic polarization (i/E) curves during nickel deposition in the absence and presence of NO_3^- ions. The curves were swept from the rest potential (-570 mV) in the negative direction at scan rate of 20 mVs^{-1} . In the absence of NO_3^- ions, the curve (curve 1) is characterized by an initial rapid potential-shift to more negative values followed by a gradual increase with increase in current density. This indicates that the deposition of nickel, in the absence of NO_3^- ions, is attended by a high activation polarization [11]. However, in the presence of NO_3^- ions, the polarization curves are characterized by the presence of a current plateau (limiting current i_{lim}) followed by a rapid rise in current at high negative potentials as a result of hydrogen evolution (curves 2–6). The magnitude of i_{lim}

Table 1. Effect of bath temperature as well as the deposition time on the CCE% of black nickel deposition

| Temp ($^\circ\text{C}$) | CCE (%) | t (min) | CCE (%) |
|---------------------------|---------|-----------|---------|
| 25 | 58 | 5 | 28 |
| 35 | 67 | 8 | 38 |
| 40 | 58.5 | 10 | 58 |
| 50 | 48.9 | 15 | 60.5 |

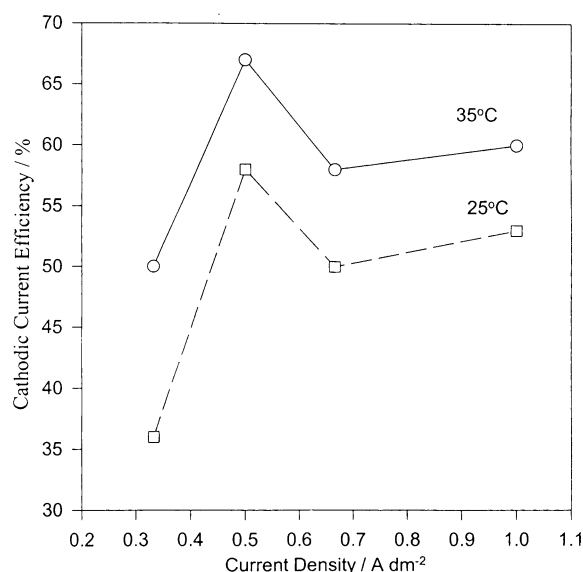


Fig. 2. Cathodic current efficiency against current density from the modified Watts bath at different temperatures.

is proportional to the concentration of NO_3^- ions as shown in Figure 3 inset.

To obtain quantitative information about the kinetics of nickel deposition in the presence of NO_3^- ions, Tafel lines were derived from the corresponding polarization curves (Figure 4). The Tafel plots were constructed using the experimental data of Figure 3. Exchange current densities, i_0 , for black nickel deposition were obtained by extrapolating the Tafel lines to zero overpotential. The calculated electrochemical kinetic parameters, Tafel slope b , the exchange current densities, i_0 , and the transfer coefficient, α , are listed in Table 2. The data indicate that Tafel slopes decrease in the presence of NO_3^- , while the transfer coefficient, α , increases with increasing NO_3^- concentration, implying that the charge transfer reaction is affected by the presence of NO_3^- . Moreover, the exchange current density, i_0 , is markedly decreased with increasing NO_3^- concentration. Generally, the exchange current density i_0 is decreased when the electrochemical reaction is inhibited [12]. This means that NO_3^- decreases the rate of Ni^{2+} ion transfer across the electrical double layer.

3.3. TP and TI of the black nickel deposition bath

The TP of the modified bath was measured using a Haring–Blum cell at 25°C , pH 4.6 and $t = 10 \text{ min}$. According to the cell geometry, the total cell current i is divided into two partial currents, i_n and i_t corresponding to the respective cathodes. In the absence of polarization, the primary current ratio (i_n/i_t) depends on the electrical resistance of the electrolyte between the anode and the respective cathodes, i.e., it is inversely proportional to the ratio of their distances from the anode. Thus the primary current ratio should be equal to the distance ratio, L . Once current passes, polarization takes place and it is assumed it will be higher at the nearer

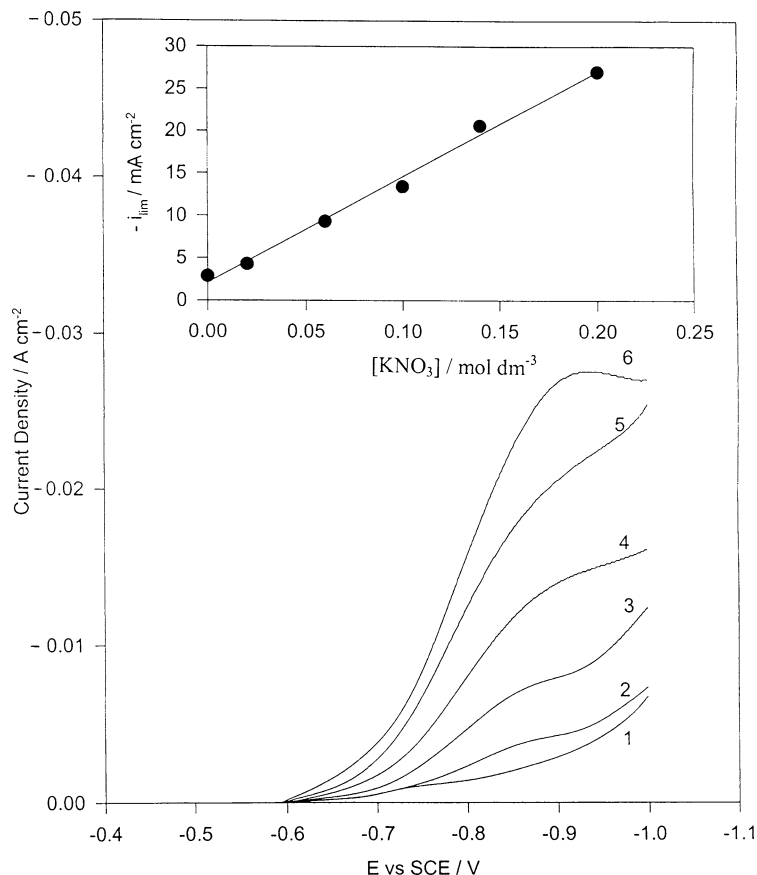


Fig. 3. Potentiodynamic cathodic polarization curves during nickel deposition in the absence of NO_3^- ions curve (1) and in presence of NO_3^- ions curves: (2) 0.02 M KNO_3 , (3) 0.06 M KNO_3 , (4) 0.1 M KNO_3 (5) 0.14 M KNO_3 and curve (6) 0.2 M KNO_3 , insert is the i_{lim} against KNO_3 concentration.

cathode than at the farther one. Because polarization resistance may be considered as being in series with the ohmic resistance, the current at the nearer cathode is decreased, giving rise to a more uniform secondary current distribution ratio. More equalization of the

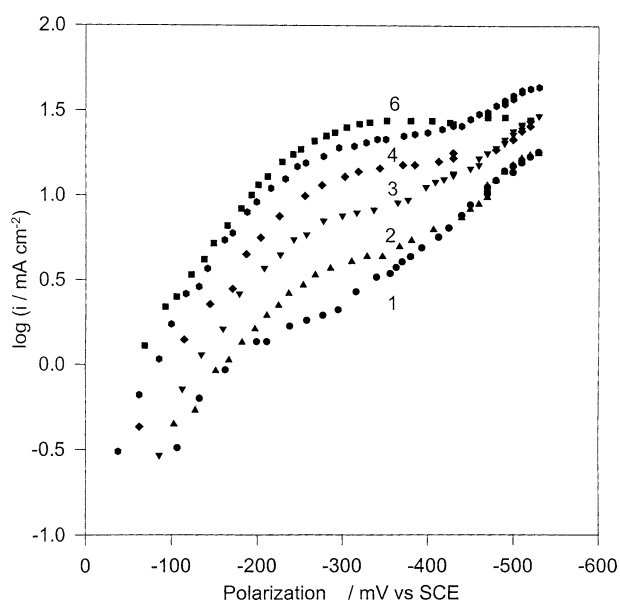


Fig. 4. Tafel plots derived from polarization curves of Fig. 3, curves: (1) 0.00 M KNO_3 , (2) 0.02 M KNO_3 , (3) 0.06 M KNO_3 , (4) 0.1 M KNO_3 (5) 0.14 M KNO_3 and curve (6) 0.2 M KNO_3 .

current ratio could be achieved by increasing the conductivity of the bath.

The TP values of this bath computed using Field's empirical formula at a distance ratio of (1:5) are shown in Table 3. Under the chosen plating conditions of $t = 10$ min, $i = 0.5 \text{ A dm}^{-2}$, Temp = 25 °C, it was found that the TP (TP = 61.0%) is higher than that reported, not only for white Ni, but also for different metals deposited under similar operating conditions from different baths [13–16]. It is worth mentioning that the highest value of TP recorded for a Watts bath is 28% in the presence of dimethylamine–borane [14]. The TP of the modified Watts bath depends strongly on bath temperature. For

Table 2. Tafel kinetic parameters obtained for nickel deposition in the presence and absence of NO_3^- ions (data obtained from polarization = -100 to -300 mV in Fig. 4 i.e. Tafel region)

| $[\text{NO}_3^-]/\text{mol}$ | Tafel slope b/V decade $^{-1}$ | Exchange current density, $i_0/\text{mA cm}^{-2}$ | Transfer coefficient (α) |
|------------------------------|----------------------------------|---|-----------------------------------|
| 0.00 | 0.24 | 6.7 | 0.13 |
| 0.02 | 0.20 | 6.6 | 0.15 |
| 0.06 | 0.17 | 5.0 | 0.17 |
| 0.10 | 0.15 | 4.3 | 0.19 |
| 0.14 | 0.17 | 1.7 | 0.17 |
| 0.20 | 0.18 | 1.2 | 0.17 |

Table 3. Effect of bath temperature on the TP as well as the TI of the modified Watts bath (pH 4.6, $i=0.5 \text{ A dm}^{-2}$, $t=10 \text{ min}$)

| Temp (°C) | TP | TI |
|-----------|-----|-----|
| 25 | 61 | 4.3 |
| 30 | 3.9 | 1.1 |

example, increasing the temperature from 25 to 30 °C decreases the TP greatly from 61 to 3.9% (Table 2).

Some linear plots between the metal distribution ratio M , and the linear ratio L (1:1–1:5) are given in Figure 5. The reciprocal of the slope of this plot is called the TI and represents a direct measure of bath TP [17]. Expressing the results in the form of TI rather than TP is advantageous because several experimental points are taken during the measurements of the TI and this minimizes measurement errors. In addition a single number, which is characteristic of a range of linear ratios, is obtained. The data of Table 3 reveal that the calculated value of TI changes in a manner almost parallel to that observed for TP.

3.4. Chronoamperometric measurements

Potentiostatic current–time transients, when used for studying the kinetics of nucleation and growth of nuclei of a metallic phase, have some advantages over cyclic voltammetry. The nucleation occurs at a constant cathodic potential, determining constant values of the nucleation work and the charge transfer rate for the entire surface of an energy-uniform electrode within a specified time period. For this purpose, a series of current–time transients at a given deposition potential, for black nickel deposition from the modified Watts bath was measured and some representative data are given in Figure 6. The decrease in current in the initial stages of the transients is related to double layer

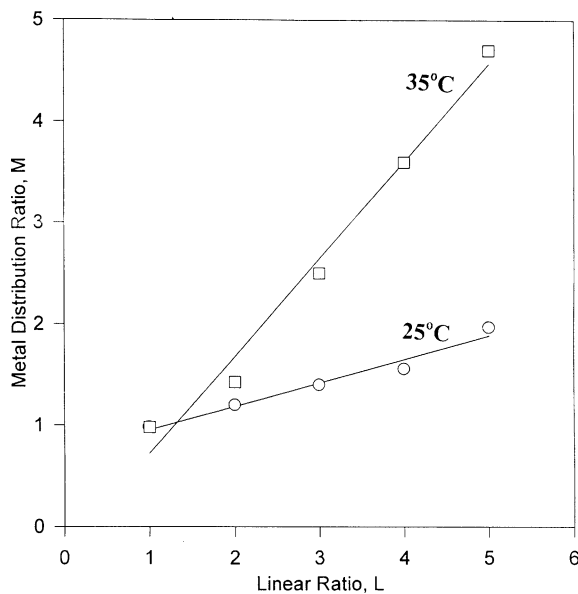


Fig. 5. Metal distribution ratio M , against linear ratio L , for the modified Watts bath at different temperatures.

charging [18]. Then the current rises to a steady-state value for a given potential, which is determined by diffusion. Moreover, the data in Figure 6 show that, as the cathodic potential is made more negative, the steady-state current value increases, suggesting that the rate of growth of nuclei is controlled by mass transfer. The most interesting part of the $i-t$ transients is the rising portion, which corresponds to the density before overlapping of the first monolayer of the growth of nuclei and therefore can be used to determine the kinetics of nuclei growth [19].

Scharifker and Hills [20] considered two types of nucleation, and proposed the following current–time relationships:

$$i = zFD^{1/2}NKt^{1/2} \quad (6)$$

$$i = zFD^{3/2}C^{1/2}AN_{\infty}K'^{3/2} \quad (7)$$

for instantaneous nucleation in which the nuclei are formed at the beginning of the pulse, and for progressive nucleation in which the nuclei are continuously formed during the crystal growth, where $K = (\pi CM/\rho)^{1/2}$, $K' = 4/3 (\pi CM/\rho)^{1/2}$, i is the current density, t is time, D is the diffusion coefficient, C is the bulk concentration, zF is the molar charge transferred during electrodeposition, M and ρ are molecular weight and density respectively, N is the total number of nuclei, A is the steady state nucleation rate constant per site and N_{∞} is the number density of active sites.

In order to classify the nucleation process as either instantaneous or progressive. Analysis of the rising part

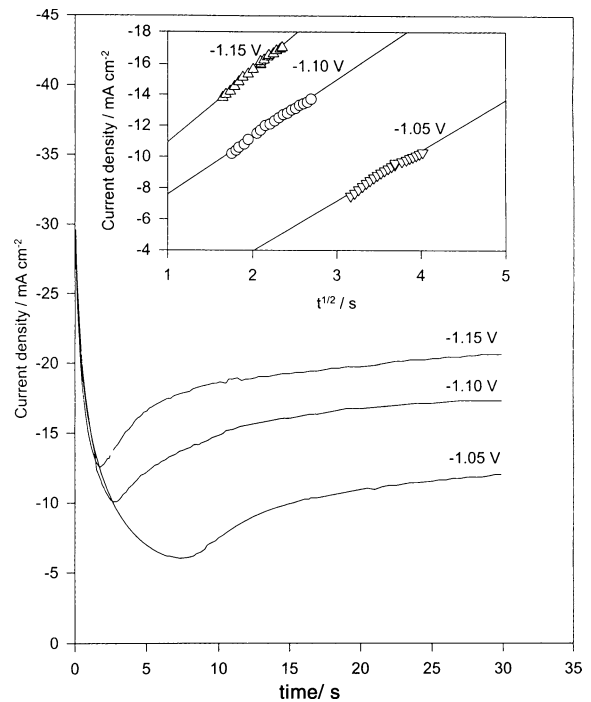


Fig. 6. Potentiostatic current–time transients from the modified Watts bath at different deposition potentials, insert is the dependence of current on $t^{1/2}$.

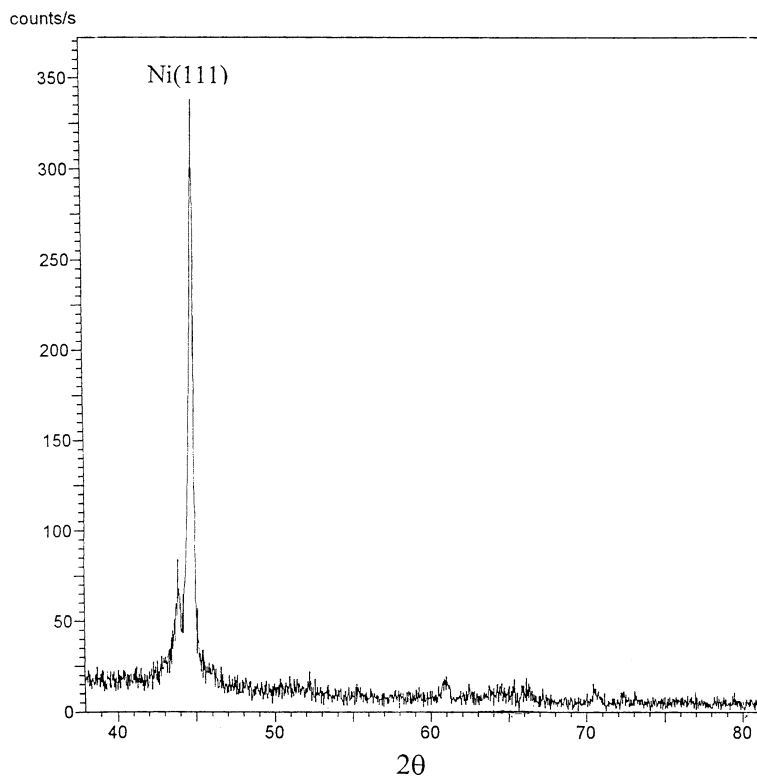


Fig. 7. XRD pattern of as-deposited black nickel from the modified Watts bath at pH 4.6, $i=0.5 \text{ A dm}^{-2}$, $T=25 \text{ }^\circ\text{C}$ and $t=10 \text{ min}$.

of transient is possible by representing, for the initial transient portion, i vs $t^{1/2}$ for instantaneous (Equation 7) and i vs $t^{3/2}$ for progressive nucleation (Equation 8). For the experimental data shown in Figure 6, plots of i vs $t^{1/2}$ show good linearity. On the other hand, plots of i vs $t^{3/2}$ show poor linearity. This indicates that under the experimental conditions, instantaneous Ni nucleation occurs (Figure 6 inset).

3.5. XRD analysis

XRD patterns of the black nickel deposited on steel substrate from the modified Watts bath at pH 4.6, $i=0.5 \text{ A dm}^{-2}$, $t=10 \text{ min}$. and at $T=25 \text{ }^\circ\text{C}$ is represented in Figure 7. In this case, Ni(111) is the preferred orientation of the black nickel deposit. This indicates that the modified Watts bath favours the crystalline growth of a deposit with Ni(111) preferred orientation. No peaks characteristic of nickel oxide were recorded, indicating that the nickel deposit is pure and does not contain oxide. In addition the patterns do not contain Ni(200) and Ni(220) phases. The work of Hu et al. [21] implies that Ni from a Watts bath with Ni(111) preferred orientation possesses a higher activity for hydrogen and oxygen evolution due to having a larger amount of active sites.

4. Conclusions

Strongly adherent thin films of black nickel can be electrodeposited on to steel by the addition of nitrate to

a Watts bath. The best operating conditions necessary to produce a highly adherent black nickel were found to be $\text{NiSO}_4 \cdot 6\text{H}_2\text{O}$ 0.63 M, $\text{NiCl}_2 \cdot 6\text{H}_2\text{O}$ 0.09 M and H_3BO_3 0.3 M and KNO_3 0.2 M at pH=4.6, $i=0.5 \text{ A dm}^{-2}$, $T=25 \text{ }^\circ\text{C}$ and $t=10 \text{ min}$. Under the chosen plating conditions of $t=10 \text{ min}$, $i=0.5 \text{ A dm}^{-2}$, $\text{Temp}=25 \text{ }^\circ\text{C}$, the TP (TP=61.0%) is higher than that reported for white Ni deposited under similar operating conditions from different baths. The potentiostatic current-time transients indicated instantaneous nucleation. XRD studies showed that the black nickel deposit consists of metallic nickel with Ni(111) preferred orientation.

References

1. F.J. Essex and D. Probert, "The Canning Handbook of Surface Finishing and Technology", (E. & F.N. Spon Ltd., New York, 1985), p. 402.
2. E. Barrera, M.P. Pardave, N. Batina and I. Gonzalez, *J. Electrochem. Soc.* **147** (2000) 1787.
3. K.M. Yousif, *Metal Finish.* **93** (1995) 90.
4. C. Anandan, V.K. William Grips, K.S. Rajam, V. Jayaram and P. Bera, *Appl. Surf. Sci.* **191** (2002) 254.
5. F. Kadirgan and M. Sohmen, *Turk. J. Chem.* **23** (1999) 345.
6. S. John, *Metal Finish.* **95** (1997) 84.
7. K.S. Indira, S.R. Rajagopalan, M.I.A. Siddiqi and K.S.G. Doss, *Electrochim. Acta* **9** (1964) 1301.
8. E.J. Serfass, R.S. Muraca and W.R. Meyer, *Am. Electroplaters' Soc.* **30** (1952) 101.
9. M.A.M. Ibrahim, *Plat. Surf. Finish.* **87** (2000) 67.
10. S. Field, *Metal Ind. (London)* **44** (1934) 416.
11. S.S. Abd El Rehim, M.A.M. Ibrahim and M.M. Dankaria, *Trans. Inst. Metal Finish.* **80** (2002) 29.

12. M.A.M. Ibrahim, D. Pongakao and M. Yoshimura, *J. Solid State Electrochem.* **6** (2002) 341.
13. M.A.M. Ibrahim, S.S. Abd El Rehim, S. M. Abd El Wahaab and M.M. Dankeria, *Plat. Surf. Finish.* **April** (1999) 69.
14. S. Wehner, A. Bund, U. Lichtenstein, W. Plieth, W. Dahms and W. Richtering, *J. Appl. Electrochem.* **33** (2003) 457.
15. M.A.M. Ibrahim, *J. Chem. Technol. Biotechnol.* **75** (2000) 745.
16. M.A.M. Ibrahim, M.A. Amin and M.A. Abbass, *Trans. Inst. Metal Finish.* **83** (2004) 105.
17. R.V. Jelin and H.F. David, *J. Electrochem. Soc.* **104** (1957) 279.
18. G. Trejo, A.F. Gil and I. Gonzalez, *J. Appl. Electrochem.* **26** (1996) 1287.
19. S. Fletcher, C.S. Halliday, D. Gates, M. Westcott, T. Lwin and G. Nelson, *J. Electroanal. Chem.* **159** (1983) 267.
20. B. Scharifker and G. Hills, *Electrochim. Acta* **28** (1983) 879.
21. C.-C. Hu, C.-Y. Lin and T.-C. Wen, *Mater. Chem. Phys.* **44** (1996) 233.